Correlated escape of active particles across a potential barrier

View Online   Export Citation   CrossMark

Lorenzo Caprini,[1,2,a)] (ID) Fabio Cecconi,[2] (ID) and Umberto Marini Bettolo Marconi[1] (ID)

AFFILIATIONS

[1] Heinrich-Heine-University of Düsseldorf, Universitätsstrasse 1, Düsseldorf, Germany
[2] Scuola di Scienze e Tecnologie, Università di Camerino, Via Madonna delle Carceri, I-62032 Camerino, Italy
[3] Istituto dei Sistemi Complessi (CNR), Via Taurini 19, I-00185 Roma, Italy

[a)]Author to whom correspondence should be addressed: lorenzo.caprini@gssi.it

ABSTRACT

We study the dynamics of one-dimensional active particles confined in a double-well potential, focusing on the escape properties of the system, such as the mean escape time from a well. We first consider a single-particle both in near and far-from-equilibrium regimes by varying the persistence time of the active force and the swim velocity. A non-monotonic behavior of the mean escape time is observed with the persistence time of the activity, revealing the existence of an optimal choice of the parameters favoring the escape process. For small persistence times, a Kramers-like formula with an effective potential obtained within the unified colored noise approximation is shown to hold. Instead, for large persistence times, we developed a simple theoretical argument based on the first passage theory, which explains the linear dependence of the escape time with the persistence of the active force. In the second part of the work, we consider the escape on two active particles mutually repelling. Interestingly, the subtle interplay of active and repulsive forces may lead to a correlation between particles, favoring the simultaneous jump across the barrier. This mechanism cannot be observed in the escape process of two passive particles. Finally, we find that in the small persistence regime, the repulsion favors the escape, such as in passive systems, in agreement with our theoretical predictions, while for large persistence times, the repulsive and active forces produce an effective attraction, which hinders the barrier crossing.

I. INTRODUCTION

Nowadays, biological systems, such as bacteria and cells, or some specific classes of colloids are classified as *active*.[1–3] They distinguish from *passive* systems for a plethora of interesting phenomena experimentally observed, which opens the way to many intriguing medical and engineering applications.[4] Active systems often accumulate near obstacles[5–7] and boundaries[8–10] and display collective phenomena such as living-clusters,[11,12] motility induced phase separation,[13–18] and spatial velocity correlations.[19–22] These properties have been reproduced with the help of coarse-grained stochastic models that neglect the biological or chemical origin of the activity in favor of an additional degree of freedom, simply referred to as the *activity* or *active force*.[23,24] This force is stochastic and imparts a typical speed to the particle, lasting for a characteristic time τ, termed persistence time. The resulting trajectories maintain, on the average, the same direction for a time of order τ, as also observed in experiments.

Recently, the behavior of active systems confined in thin geometries or by external potentials has been a matter of intense investigation[25–31] through both experimental and numerical studies. For instance, active colloids could be confined in external potentials using magnetic or optical tweezers[32] and recently by using acoustic traps,[33] while the confinement for Hexbug particles, i.e., macroscopic self-propelled toy robot, could be simply achieved through a parabolic dish.[34] Some approximate theoretical treatments have been formulated to predict the statistical properties of active systems.[35] These include the diffusion properties in complex environments,[36,37] the probability distribution function (displaying strong deviation from Boltzmann profiles),[38,39] the pair correlation functions,[40,41] the pressure, and the surface tension.[42] However, these methods usually work in specific ranges of parameters and, in some cases, break down in regimes of strong or persistent activities. This failure is found, for instance, in the active version of the celebrated Kramers' problem[43,44] concerning the escape from a potential barrier. In this context, a paradigmatic case that has received

much attention in the literature of passive particles concerns the escape in a double-well potential. In the active case, some analytical results have been obtained in near equilibrium regimes,[45–47] where the average escape time can be analytically predicted by taking advantage of equilibrium-like approximations. Subsequently, most of the studies have been focused on far-from-equilibrium regimes (large swim velocities and/or large persistence times) showing behaviors without passive counterparts: for instance, Woillez *et al.* found that the escape time of active particles is affected by the whole shape of the potential and not only by the height of the potential barrier.[48] In addition, some properties of the escape mechanism have been discussed in Ref. 49 for large persistence regimes, where the velocity distribution of particles around the potential barrier exhibits a bimodal shape, indicating that the barrier crossing occurs almost deterministically at variance with the case of passive particles.

An estimate of the escape rate from a well in the limit of infinite persistence is given in Ref. 50 by using large-deviation techniques, showing that the escape rate does not depend on the barrier height of an effective potential but depends on the maximal force exerted on the particle inside the trap. Still in the same limit, Fily[51] obtained an approximate expression for the probability distribution, predicting a vanishing density in the regions where the potential is concave and a nonlocal dependence of the density on the external potential. Finally, Debnath and Ghosh[52] focused on the escape time in two dimensions and in the presence of hydrodynamic interactions of an active Brownian particle carrying a passive cargo.

The interest in the active escape processes goes beyond the paradigmatic case of the double-well potential as testified by the studies on the escape from other potential shapes,[53,54] for instance, harmonic potentials[55,56] with interesting applications for the active version of the trap model[57] or the escape behavior of active particles in rugged energy landscapes,[58] reminiscent of active glasses.[59–63] It is important to remark that theoretical results for the mean escape time in the presence of general potentials have been only derived in the limit of small active force.[64] Finally, recent works have studied the escape of active particles from thin openings of confining geometries, such as disks,[65–67] for their potential applications in biological processes.[68] The average escape time has been investigated also in simpler geometries, such as one-dimensional channels,[69] open-wedge channels,[70] and channels with bottlenecks,[71] suitable to model the escape of living organisms from biological pores.

In this paper, we focus on the escape properties of active particles, evaluating small, intermediate, and large persistence, and find the occurrence of an optimal persistence favoring the escape from the potential barrier. In the second part of the work, the same problem is addressed by considering a system formed by two interacting active particles to assess the effect of repulsive interactions on the escape process. The paper is structured as follows: In Sec. II, we introduce the model used to simulate the dynamics of active particles, while in Secs. III and IV, we study the escape problem for one and two interactive particles, respectively. In Sec. V, we present the conclusions.

II. MODEL

We consider the dynamics of active particles confined in an external double-well potential of the form

$$W(x) = \frac{W_0}{4}\left(x^2 - a^2\right)^2. \tag{1}$$

The profile of $W(x)$ is characterized by two minima at $x = \pm a$ separated by a potential barrier at $x = 0$ of height $W_b = W_0 a^4/4$. The dynamics is made *active* by including a stochastic force, f_i^a, in the evolution for the particle position x_i. f_i^a is generated by an Ornstein–Uhlenbeck process and is characterized by a persistence time τ and a variance v_0. This choice corresponds to the so-called active Ornstein–Uhlenbeck particles (AOUP) model[35,72–77] and reproduces the typical phenomenology of active particles.[38,78,79] The AOUP has been often employed as an approximation for other popular active models[80–82] or to describe the behavior of a colloidal particle in a bath of active particles.[83–85] The equations of motion for N overdamped AOUP with the position x_i are given by

$$\gamma \dot{x}_i = f_i^a - W'(x_i) + F_i, \tag{2a}$$

$$\tau \dot{f}_i^a = -f_i^a + \gamma v_0 \sqrt{2\tau}\xi_i, \tag{2b}$$

where ξ_i is the white noise with a zero average and unit variance such that $\langle \xi_i(t)\xi_j(0)\rangle = \delta_{ij}\delta(t)$ and γ is the friction coefficient. Finally, the last force term in Eq. (2), namely $F_i = -\partial_{x_i} U_{tot}$, is due to the repulsive interactions between neighboring particles and models volume exclusion. This force corresponds to the potential $U_{tot} = \sum_{i<j} U(|x_j - x_i|)$, where U is a Weeks–Chandler–Andersen (WCA) potential of the form

$$U(r) = \begin{cases} 4\epsilon\left[\left(\dfrac{\sigma}{r}\right)^{12} - 2\left(\dfrac{\sigma}{r}\right)^6 + 1\right], & r \leq \sigma, \\ 0, & r > \sigma, \end{cases} \tag{3}$$

where $r = |x_i - x_j|$ is the distance between the two particles, σ is the nominal particle diameter, and ϵ is the typical energy scale of the interaction; for simplicity, we set $\sigma = 1$ and $\epsilon = 1$.

III. ONE-PARTICLE ACTIVE ESCAPE PROBLEM

Before delving into the case of two particles, we consider a single-particle, i.e., the dynamics (2) with $N = 1$. In this section, for simplicity, we omit Latin subscripts.

In the one-particle case, Refs. 49 and 50 have already shown that the jump mechanism from a potential well to the other is strongly affected by the persistence time τ, which can change also qualitatively the dynamical picture of the escape process. Roughly speaking, we can distinguish two limiting mechanisms, depending on the values of τ considered: (i) the regime of small τ such that f^a relaxes faster than the particle position, x, and (ii) a regime of large persistence such that f^a relaxes slower than x.

A. Small persistence regime

When f^a relaxes faster than x (namely, in the regime of small τ), the system is near the equilibrium and the unified colored noise approximation (UCNA) applies.[35,86,87] This means that the role of the active force can be recast onto an effective potential with an

effective diffusion coefficient $D_a = v_0^2 \tau$. In practice, the active particle behaves as a Brownian-like particle described by the probability distribution

$$p(x) \propto \exp[-H(x)/D_a\gamma], \qquad (4)$$

where $H(x)$ is the following effective potential:[87]

$$H(x) = W(x) + \frac{\tau}{2\gamma}\left(W'(x)\right)^2 - D_a\gamma \log\left(1 + \frac{\tau}{\gamma}W''(x)\right), \qquad (5)$$

where the prime denotes the spatial derivative. $H(x)$ can be interpreted as the Hamiltonian of a passive particle, depending on $W(x)$ and its derivatives. The extra terms in Eq. (5) maintain the symmetric two-well structure [see Fig. 1(a) illustrating $H(x)/D_a\gamma$ for two different values of τ] but shift the positions of the two minima, $|x_m|$, and change the height of the effective potential barrier, $H_b = H(0) - H(|x_m|)$. To first order in τ, we obtain

$$|x_m| \simeq a\left(1 + 3\frac{D_a\tau}{a^2}\right), \qquad (6a)$$

$$H_b \simeq \frac{a^4 W_0}{4}\left(1 + 12\frac{D_a\tau}{a^2}\right). \qquad (6b)$$

The height of the potential barrier increases with the activity; thus, one would expect that a larger activity hinders the passage from one well to the other. On the contrary, since the key factor controlling the escape dynamics is the ratio $H_b/D_a\gamma = H_b/(v_0^2\tau\gamma)$, which decreases with τ (and v_0), one finds that the active force favors the escape process [as shown in Fig. 1(a)]. In summary, in the small persistence regime, the jump process resembles its passive counterpart and the average escape time, t_e, can be estimated by applying the Kramers formula[88] by considering the effective potential (5),

$$t_e \approx \frac{2\pi}{\sqrt{H''(|x_m|)\,|H''(0)|}}\exp\left(\frac{H_b}{D_a\gamma}\right), \qquad (7)$$

where H'' denotes the second derivative of Eq. (5) and, as usual, formula (7) holds when $H_b/(D_a\gamma) \gg 1$. As a matter of fact, in the regime of small τ, the leading term in the expression (5) is simply the potential $W(x)$ while the remaining terms provide small corrections whose relevance increases as τ grows. As a consequence, for τ small enough [when $O(\tau)$ is negligible in the expression for $H(x)$], Eq. (7) reduces to

$$t_e \sim \exp\left[W_b/(v_0^2\tau\gamma)\right], \qquad (8)$$

which mainly depends on the height W_b of the potential barrier, showing that t_e exponentially decreases when τ or v_0 is increased.

Predictions (7) and (8) have been checked numerically, as shown in Fig. 1(b), where the escape time t_e is plotted as a function of τ for two different values of v_0. As expected from the naive passive-like formula (8), t_e decreases as τ grows, and similarly, it becomes smaller as v_0 increases. However, a quantitative agreement in a wide τ-range is achieved only by using the UCNA result (7), whereas Eq. (8) fails at larger values of τ.

B. Large persistence regime

In the case where f^a relaxes slower than x, which is in a regime of large persistence, we can identify a jump mechanism differing from that of a passive particle.[49] In fact, if τ exceeds a certain threshold, the UCNA distribution (4) becomes ill-defined as the argument of the logarithm

$$\log\left(1 + \frac{\tau}{\gamma}W''(x)\right)$$

in Eq. (5) becomes negative for certain values of x. At large enough value of τ, this occurs because $W''(x) < 0$ for $|x| < a/\sqrt{3}$. Nevertheless, even for large τ, as shown in Ref. 49, around the potential minima, the particle distribution can be fairly well represented by $p(x) \propto e^{-H(x)/D_a\gamma}$. Moreover, Ref. 49 shows that in the regime of large τ, the jump process occurs almost deterministically when the modulus of the active force $|f_a|$ exceeds the threshold
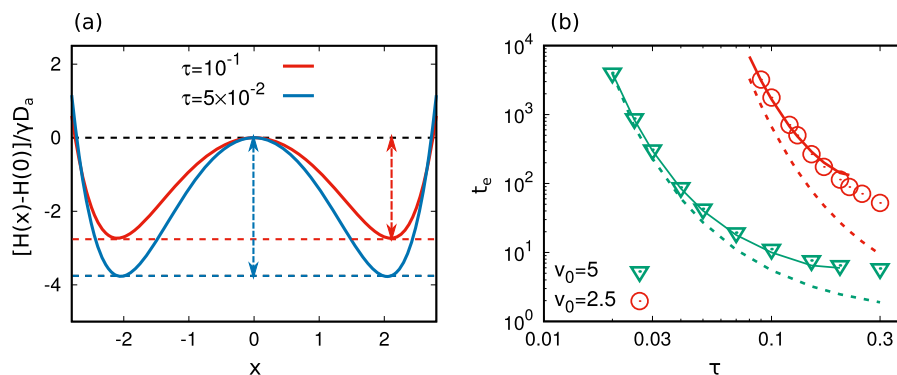
FIG. 1. Panel (a): Effective potential, $(H(x) - H(0))/\gamma D_a$, where $D_a = v_0^2\tau$, for $\tau = 10^{-1}$ (red curve) and $\tau = 5 \times 10^{-2}$ (blue curve). Horizontal dashed lines are guides for the eyes, marking the value of the maximum and minima of the effective potential, while vertical dashed arrows measure the height of the effective potential barrier, $H_b/(D_a\gamma)$. Panel (b): average escape time, t_e, as a function of the persistence time τ for two different values of the swim velocity v_0. Colored points are the results of numerical simulations, solid lines are obtained from Eq. (7), and dashed lines are from Eq. (8). We remark that the prediction (7) is shown for those values of τ for which the UCNA prediction is defined. The other parameters of the simulations are $W_0 = 1$ and $a = 2$.

$f_M = 2W_0 a^3/(3\sqrt{3})$ corresponding to the maximal force exerted by the double-well (i.e., the modulus of the force evaluated at the inflection points $\pm a/\sqrt{3}$). In particular, jumps from the left (right) well to the right (left) one occur when $f_a > f_M$ ($f_a < -f_M$). These results have been formalized using large-deviation techniques in Ref. 50, where an asymptotic expression for the distribution function, $p(x)$, has been derived in the limit $\tau \to \infty$.

To understand how the escape properties are modified by a persistent active force, we study the average escape time, t_e, as a function of τ and explore values for which UCNA does not hold. In particular, Fig. 2(a) shows t_e vs τ for different values of the swim velocity, v_0. For each value of τ, the larger the value of v_0, the larger the value of t_e. Instead, as a function of τ, a non-monotonic behavior is observed. After a first decrease, which resembles the Kramers-like behavior (8) described in the small τ regime, the escape time drops to a minimum for $\tau = \tau_m$ until to increase at larger values of τ. This means that for a given potential setup and swim velocity, one can identify an optimal value of the persistence time (τ_m) favoring the jump process. The above scenario can be explained by a simple argument based on the interplay between the persistence length $\ell = v_0 \tau$ and the distance, a, between the maximum and the minimum of the potential. When $\ell \ll a$, the active force changes direction several times during the barrier climbing. Thus, the active particle behaves as a passive one in a thermal bath of effective temperature $\gamma v_0^2 \tau$ and confined by an effective double-well potential. As already discussed in Fig. 1, t_e decreases as τ grows. Instead, when $\ell \gg a$, the escape occurs almost deterministically when the active force overcomes f_M because f^a has a little chance to reverse its direction during the barrier crossing at variance with the small-τ regime. Thus, for $\ell \gg a$, the barrier crossing is actually related to a first passage for the process (2b): the larger the value of τ, the larger the time waited for the occurrence of a value of the active force such that $f_a > f_M$, implying a larger t_e. As a consequence, we expect the presence of a minimum in the intermediate regime, say $\ell = v_0 \tau \sim a$. The argument explains the behavior of τ_m with the swim velocity; indeed,

as shown in Fig. 2(a), τ_m decreases with v_0 in agreement with the scaling,

$$\tau_m \sim \frac{a}{v_0}.$$

We remark that the non-monotonic behavior with τ has been already observed in other observables of this system, such as the entropy production[89] or the integrated linear response to a small perturbation, introduced to test the breakdown of the detailed balance.[90]

As reported by Fig. 2(a), the increase in t_e with τ for $\tau > \tau_m$ is quite slow and displays an algebraic growth, which roughly approaches a linear dependence $t_e \sim \tau$ in the regime $\tau \gg \tau_m$. This qualitative observation can be supported by a theoretical argument holding in the limit $\tau \to \infty$. As already discussed, since for $\tau \gg \tau_m$, a jump occurs only when $f^a > f_M$ (or $f^a < -f_M$), we can identify t_e as the typical time taken by f^a to reach f_M (or $-f_M$), which is nothing but the first passage problem of an Ornstein–Uhlenbeck (OU) process. This is briefly reviewed in Appendix (see also Ref. 91) and provides the following prediction:

$$\lim_{\tau \to \infty} t_e \approx \tau \sqrt{\pi} \int_0^\phi du \; e^{u^2} (1 + \text{Erf}[u]), \qquad (9)$$

where $\phi = f_M/\sqrt{2} v_0 \gamma$ is a dimensionless force and $\text{Erf}[\cdot]$ indicates the error function. As shown in Fig. 2(a) (see the dashed colored lines), the prediction (9) is in fair agreement with data (except for the presence of an extra factor $\sqrt{2}$, which is missed by our theory) and, in particular, allows us to explain the behavior $t_e \propto \tau$ observed by simulations for $\tau \gg \tau_m$. In addition, the saddle-point method, applied to Eq. (9) for $f_M \ll v_0 \gamma$, yields the expression

$$\lim_{\tau \to \infty} t_e \approx \tau \frac{f_M}{v_0 \gamma} \sqrt{\frac{\pi}{2}} \exp\left(\frac{f_M^2}{2 v_0^2 \gamma^2}\right), \qquad (10)$$
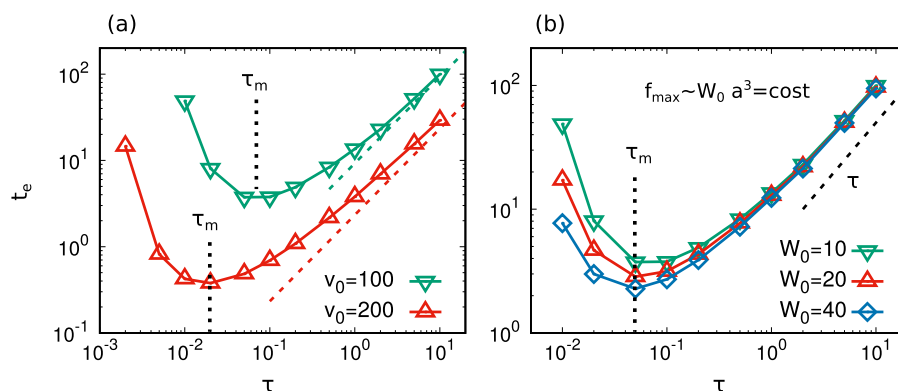
FIG. 2. Average escape time, t_e, as a function of the persistence time τ for two different values of the swim velocity $v_0 = 10^2, 2 \times 10^2$ (with a fixed potential) in panel (a) and by keeping fixed v_0 and by changing the potential parameter in panel (b). In particular, in the latter case, t_e is shown for three different values of the potential strength $W_0 = 10, 20, 40$ by keeping fixed the maximal force exerted in the flex point, $f_M \sim W_0 a^3$. The colored dashed lines in panel (a) are obtained by using Eq. (9) with the values of v_0 indicated in the legend. Instead, the dashed black line in panel (b) qualitatively shows the linear scaling with τ. Finally, the dotted black lines are eye-guides, which mark the value of τ_m The other parameters of panel (a) are $W_0 = 10$ and $a = \sqrt{10}$, while the other parameters of panel (b) are $v_0 = 10^2$ and a scaling accordingly to the value of W_0 such that $W_0 a^3 = 10^{5/2}$.

which coincides with the result of Ref. 50 except for the prefactor depending on τ, which has not been derived by Woillez *et al.* From Eqs. (9) and (10), the difference with the passive escape problem is contained in the scaling of t_e with the parameter of the potential. Indeed, the average escape time of a passive Brownian particle mainly depends on the height of the potential barrier, which scales as $W_0 a^4/4$ for the double-well given by Eq. (1). Instead, in the active persistent case, in particular, in the regime of large τ such that $\ell \gg a$ (so that $\tau \gg \tau_m$), the escape time depends on the value of the maximal force $f_M = 2W_0 a^3/(3\sqrt{3})$ experienced along the barrier climbing. This scaling is checked in Fig. 2(b), where t_e is shown as a function of τ at fixed v_0, by varying a and W_0 such that $W_0 a^3 = \text{const}$ to keep f_M constant. In particular, we plot three different values of W_0 showing the collapse of the curves when $\tau \gg \tau_m$. This also confirms that the active escape does not depend on the height of the barrier.

IV. TWO-PARTICLE ACTIVE ESCAPE PROBLEM

In this section, we consider the dynamics (2) with $N = 2$ particles to understand the impact of the inter-particle interactions on the escape process in the double-well potential (1). For this reason, we kept constant the parameters of the potential and the swim velocity, v_0, whose roles have been already analyzed and understood in Sec. III B.

As in the single-particle case, we first describe the regime of small τ, where we expect the system to behave as a passive one with an effective potential, and then the large τ regime.

A. Small persistence regime

In analogy with Eq. (5), we can express the joint probability distribution $p_2(x_1, x_2)$ for the position of the two particles in the small-τ regime as

$$p_2(x_1, x_2) \propto \exp[-H_{tot}(x_1, x_2)/D_a \gamma], \qquad (11)$$

where $H_{tot}(x_1, x_2)$ is an effective Hamiltonian, which can be decomposed as

$$H_{tot}(x_1, x_2) = H(x_1) + H(x_2) + H_{int}(x_1, x_2). \qquad (12)$$

The term H is the single-particle effective Hamiltonian (which depends only on the external potential and its derivatives) already introduced in Eq. (5), while H_{int} is the interaction Hamiltonian (containing the inter-particle potential, U) that reads

$$H_{int} \approx \frac{\tau}{\gamma} \Big[(\partial_{x_1} U)^2 + (\partial_{x_2} U)^2 + 2(\partial_{x_1} U)\partial_{x_1} W(x_1)$$
$$+ 2(\partial_{x_2} U)\partial_{x_2} W(x_2) \Big] - D_a \gamma \log\left(1 + 2\frac{\tau}{\gamma}\partial_{x_1}^2 U\right). \qquad (13)$$

Notice that the last term follows from the approximation of the determinant of the Hessian matrix appearing in the UCNA distribution. Since $\partial_{x_1}^2 U = \partial_{x_2}^2 U$, the Hamiltonian H_{int} is invariant for $x_1 \to x_2$ and $x_2 \to x_1$, as one expects. For further details about this result in the interacting (two-particles) case, see Ref. 40. We remark that H_{int} not only depends on the interaction potential (as usual in

passive systems) but also on the external potential and their derivatives, which produce the effective attraction qualitatively responsible for cluster formation and motility induced phase separation[81] (see also Ref. 92 for the parameter range for the application of such a method).

In virtue of these analytical results for p_2, it is possible to find an effective description for a tagged particle (namely, particle 1) by integrating out the coordinate of the second particle, x_2, in Eq. (11). Applying this procedure, we obtain the expression for the single-particle marginal probability distribution, $p_1(x_1)$, from which the single-particle effective Hamiltonian is derived by taking the logarithm as follows:

$$H_{\text{eff}}(x_1) = H(x_1) - D_a \gamma \log \int dx_2 \, \exp\left(-\frac{H_{int}(x_1, x_2) + H(x_2)}{D_a \gamma}\right), \qquad (14)$$

where we recall that $D_a = v_0^2 \tau$. At this stage, Kramers' formula (7) can be easily applied by replacing H with H_{eff} to derive an analytical expression for the effective escape time t_e^{int} for the tagged particle in the interacting system.

In Fig. 3, t_e^{int} is numerically studied as a function of τ (only small values of τ are shown) and the results are compared with the Kramers-like theoretical prediction. As in the one-particle case, the agreement is fairly good for the smaller values of τ, while the theoretical prediction underestimates the numerical value of t_e^{int} when τ is increased. Figure 3 also reports the comparison between t_e^{int} and t_e (the escape time from the double-well potential in the non-interacting case). As it occurs in passive systems, we see that $t_e^{\text{int}} < t_e$. This result can be easily explained because the interaction potential decreases the effective potential barrier of the single-particle. Indeed, as long as the particles are placed in different wells, the escape follows the rules of the non-interacting problem. Instead, when the particles are placed in the same well, for instance, the left one, the right particle can escape more easily with respect to a non-interacting particle because it is roughly placed at $x_m^{int} \approx -a + \sigma$ [see also Fig. 4(a)], and thus, the single-particle effective potential barrier is reduced with respect to the bare value $W_b = W_0 a^4/4$. We also observe that as the
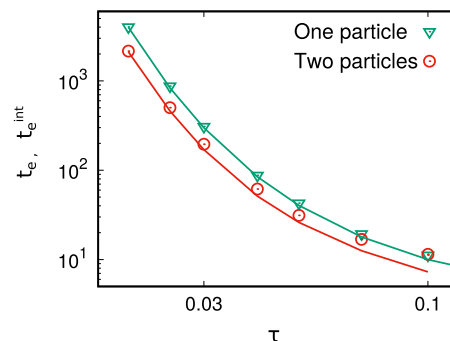
FIG. 3. Average escape time, t_e (one particle) and t_e^{int} for the one-particle system (green triangles) and the two-particle system (red circles), as a function of the persistence time τ. Colored solid lines are obtained by the theoretical predictions (7) (green line) and by Eq. (7) with $H \to H_{\text{eff}}$, where H_{eff} is obtained by Eq. (14). The other parameters of the simulations are $v_0 = 5$, $W_0 = 1$, $a = 2$, $\epsilon = 1$, and $\sigma = 1$.
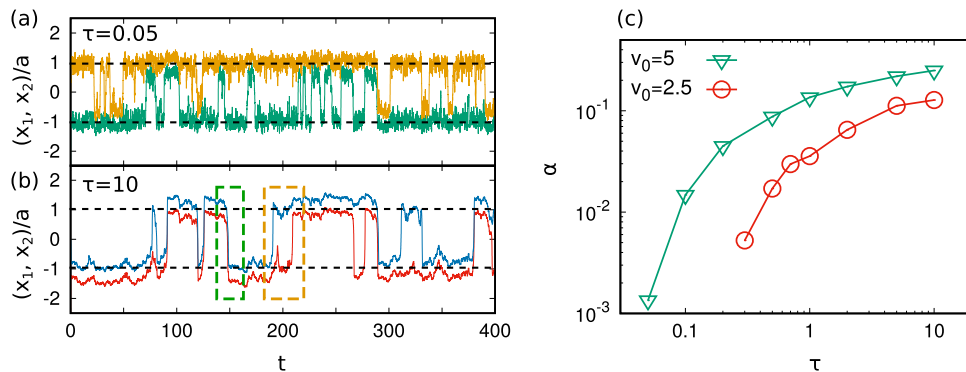
FIG. 4. Panels (a) and (b): time trajectories of the two particles (normalized by a), namely, $x_1(t)/a$ [green line in panel (a) and red line in panel (b)] and $x_2(t)/a$ [yellow line in panel (a) and blue line in panel (b)]. Panels (a) and (b) are obtained with $\tau = 0.05, 10$, respectively, with $v_0 = 5$. In both panels, the two dashed black lines mark the positions of the minima. The green dashed rectangle is drawn in correspondence of a simultaneous jump while the yellow one in correspondence of two independent jumps. Panel (c): fraction of simultaneous jump, α, as a function of τ for two different values of the swim velocity, $v_0 = 2.5, 5$. The other parameters of the simulations are $W_0 = 1$, $a = 2$, $\epsilon = 1$, and $\sigma = 1$.

persistence is increased, the difference between t_e and t_e^{int} reduces until $t_e^{\text{int}} \approx t_e$. This occurs because the interaction Hamiltonian, H_{int}, contains effective attraction terms whose relevance increases when the persistence time grows.[40] These effective attractive terms hinder the escape from a well, similarly to the real attraction in passive systems, see, e.g., Ref. 93, for the case of two particles interacting via a harmonic force, forming a dimer.

B. Large persistence regime

As we expect, the UCNA prediction (13) cannot work in the large persistence regime like in the one-particle case. In the absence of a theoretical picture, we resort to numerically study the active escape properties. Before delving into the study of the mean escape time, we focus on the phenomenology of the escape process to understand the difference between small and large persistence regimes. Figures 4(a) and 4(b) show the single-particle trajectories, namely, the positions of the two particles, $x_1(t)$ and $x_2(t)$ normalized by a as a function of time. In the two panels, two different values of τ are considered as illustrative cases for the two regimes. In the small persistence regime [Fig. 4(a)], it is not surprising that the two particles perform uncorrelated jumps so that each particle independently escapes from a well as it occurs in a system of two passive particles. Instead, in the large persistence regime, the escape process is quite different, as shown in Fig. 4(b), because among the escape events, there is a non-negligible fraction of jumps involving both particles whereby they cross the barrier almost simultaneously (see the dashed green rectangle). We refer to these events as correlated jumps. Let us suppose that the particles are both in the left well, $x_1 < x_2 < 0$. The active particle "1," which is farther from the barrier $x = 0$, could be able to drag the particle "2" toward $x = 0$, forcing its escape even if the active force of "2" is smaller than f_M, thus producing a simultaneous jump. To make this picture more quantitative, in Fig. 4(c), we measure the fraction, α, of correlated jumps occurring in a long-time simulation run as a function of τ for two different values of v_0. This fraction is defined as $\alpha = n_s/n_{tot}$ being n_s the number of simultaneous jumps and n_{tot} the total number of jumps

occurring in the time-window of the run. As expected, α is an increasing (monotonic) function of τ: the larger is the persistence, the more probable the occurrence of a correlated jump. Interestingly, depending on the value of v_0, the fraction α could reach also large values so that even the 10% or 20% of the escape events could be simultaneous. This correlated-escape scenario does not have a passive counterpart, since in that case the probability of observing a simultaneous jump is always negligible. However, correlated jumps have been observed in granular systems, where dissipative collisions determine a kind of "effective" attraction similar to that discussed in this paper.[94]

Finally, Fig. 5 shows the average escape times, t_e^{int} and t_e, for the interacting and non-interacting cases, respectively, as a function of τ, exploring also values of τ outside the applicability of UCNA. Both the escape times decrease until a minimum is reached, and then, for further values of τ, they monotonically increase. We remark that at variance with the small-τ regime, now we observe $t_e^{\text{int}} > t_e$. This
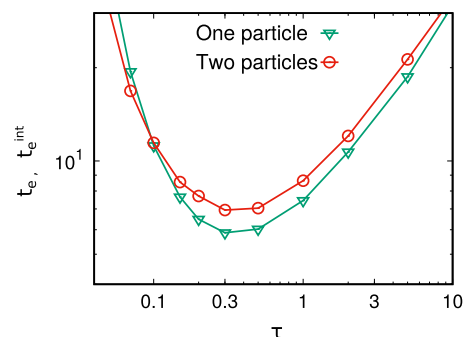
FIG. 5. Average escape time, t_e (one particle) and t_e^{int} for the one-particle system (green triangles) and the two-particle system (red circles), as a function of the persistence time τ. Solid lines are guides for the eyes. The other parameters of the simulations are $v_0 = 5$, $W_0 = 1$, $a = 2$, $\epsilon = 1$, and $\sigma = 1$.

scenario could be explained by the well-known slow-down due to the interplay between the active and repulsive forces, which concur to produce an effect qualitatively similar to an effective attraction. This mechanism hinders the escape process with respect to the non-interacting case.

V. CONCLUSION

In this paper, we have studied the escape properties of active particles—using the active Ornstein–Uhlenbeck model—confined in a double-well potential with a particular focus on the mean escape time from a well. At first, we have investigated the escape of a single-particle, considering a wide range of persistence regimes of the active force. Interestingly, we have observed the existence of an optimum value of the persistence time (at fixed external potential), which minimizes the mean escape time. We have also developed a theoretical explanation for the behavior at the small persistence regime, combining the Unified Colored Noise approximation (UCNA) with a Kramers-like theory. We have also proposed a simple theoretical argument to explain the linear growth of the mean escape time in the large persistence regime.

As a second step, we have considered a system of two active particles interacting via a repulsive potential. In addition, for so this case, we derive a theoretical prediction for the average escape time, holding in the small persistence regime: as expected for passive particles, the escape is favored in the interacting system because each particle behaves as if it was affected by an effective barrier lower than the barrier of the external potential. Interestingly, in the large persistence regime, we observe the opposite: the interplay between the active force and the repulsive interaction induces an effective attraction between the particles, which hinders the escape process in the two-particle systems. In addition, we outline the peculiar properties of the two-particle active escape: in the regime of large persistence, we observe a large fraction of simultaneous jumps (which occurs when the two particles jump together) that does not have a passive counterpart.

Recently, Brückner et al. have performed intriguing experiments of strongly confined active particles: they consider epithelial (even cancerous) cells in a simple geometry consisting of two adhesive sites connected by a thin constriction.[95–97] The cell, which has a certain degree of persistence, migrates from a site to the other and seems to behave as if it is subject to a double-well potential along with the travel direction. The results of these experiments, in particular, the position–velocity phase space and the features of the jump mechanism, are in qualitative agreement with simulations using the active Ornstein–Uhlenbeck model in a double-well potential, which shows a bifurcation-like scenario in the proximity of the potential maximum.[49] By such an analogy, we believe that our work could stimulate future experimental and numerical studies focused on the escape properties (i.e., the time that a cell needs to cross a thin constriction) and shed light on the jump properties of such an experimental system.

We expect that the phenomenology observed in this paper remains almost unchanged by considering different models for the active force, mostly for what concerns the active Brownian particle (ABP) model. Indeed, there is evidence that the ABP and the AOUP share a similar phenomenology and that the latter can be used to

derive analytical results holding for the former in some regimes of parameters.[26,81,98] Of course, the extension of the present study to a system formed by more than two particles in two dimensions could be more challenging. In this case, we expect that the clustering and the slowing down typical of interacting systems of active particles in the large persistence regime hinder the barrier crossing, while intuitively, the repulsive interactions should favor the escape process in the small persistence regime, as in the two-particle case.

AUTHOR DECLARATIONS

Conflict of Interest

The authors have no conflicts to disclose.

DATA AVAILABILITY

The data that support the findings of this study are available from the corresponding author upon reasonable request.

APPENDIX: DERIVATION OF EQ. (9)

In this Appendix, we derive the expression (9) for the escape time t_e, holding in the limit of $\tau \to \infty$. As also discussed in Sec. III, in this regime of τ, t_e can be determined by the mean first passage time taken by the active force f^a to overcome the threshold $|f_M|$ (namely, the maximal force experienced by a particle in climbing the barrier). According to the first passage theory (see Ref. 99), this time is related to the survival probability, $S(f^a, t)$, by the integral[88]

$$T(f^a) = \int_0^\infty dt \, S(f^a, t).$$

By definition, $S(f^a, t)$ is the probability that the process has not yet reached $f_{\max}$ at time t. $S(f^a, t)$ is known to satisfy the backward Fokker–Planck equation,[88] which for the OU process reads

$$\frac{\partial S}{\partial t} = -\frac{f^a}{\tau} \frac{\partial S}{\partial f^a} + \frac{(\gamma v_0)^2}{\tau} \frac{\partial^2 S}{\partial (f^a)^2} \tag{A1}$$

with the boundary conditions $S(f_{\max}, t) = 0$. In the following, for the sake of concision, we set $a = (\gamma v_0)^2$. To obtain a differential equation for $T(f^a)$, it is sufficient to integrate Eq. (A1) in the interval $0 \le t < \infty$, and taking into account that $S(f^a, \infty) = 0$ and $S(f^a, 0) = 1$, we get

$$-f^a \frac{\partial T}{\partial f^a} + a \frac{\partial^2 T}{\partial x^2} = -\tau, \tag{A2}$$

which has to be solved with the boundary conditions $T(f_{\max}) = 0$ and $T'(-\infty) = 0$. The first condition states that a process started at the boundary f_M is instantaneously absorbed, and the second one states that $f^a = -\infty$ acts as a reflecting barrier, since the very large

f^a-values are practically inaccessible due to the quadratic form of the potential, $f^2/2\tau$. The solution of Eq. (A2) can be obtained by quadrature, setting $T'(f) = w(f)$, and reads

$$T(f^a) = \frac{\tau}{a} \int_{f^a}^{f_M} dx\, e^{x^2/(2a)} \int_{-\infty}^{x} dy\, e^{-y^2/(2a)}.$$

After performing the integration on y, one obtains

$$T(f^a) = \tau \sqrt{\frac{\pi}{2a}} \int_{f^a}^{f_M} dx\, e^{x^2/(2a)} \left(1 + \mathrm{Erf}\left[\frac{x}{\sqrt{2a}}\right]\right). \tag{A3}$$

Finally, by evaluating the expression (A3) at $f^a = 0$ and after a change of the variable in the integration, we obtain Eq. (9), since $T(f^a = 0) = t_e$.

REFERENCES

[1] C. Bechinger, R. Di Leonardo, H. Löwen, C. Reichhardt, G. Volpe, and G. Volpe, Rev. Mod. Phys. **88**, 045006 (2016).

[2] M. C. Marchetti, J. F. Joanny, S. Ramaswamy, T. B. Liverpool, J. Prost, M. Rao, and R. A. Simha, Rev. Mod. Phys. **85**, 1143–1189 (2013).

[3] J. Elgeti, R. G. Winkler, and G. Gompper, Rep. Prog. Phys. **78**, 056601 (2015).

[4] G. Gompper, R. G. Winkler, T. Speck, A. Solon, C. Nardini, F. Peruani, H. Löwen, R. Golestanian, U. B. Kaupp, L. Alvarez et al., J. Phys.: Condens. Matter **32**, 193001 (2020).

[5] G. L. Miño, M. Baabour, R. Chertcoff, G. Gutkind, E. Clément, H. Auradou, and I. Ippolito, Adv. Microbiol. **8**, 451 (2018).

[6] C. Maggi, F. Saglimbeni, M. Dipalo, F. De Angelis, and R. Di Leonardo, Nat. Commun. **6**, 7855 (2015).

[7] L. Angelani, R. Di Leonardo, and G. Ruocco, Phys. Rev. Lett. **102**, 048104 (2009).

[8] I. D. Vladescu, E. J. Marsden, J. Schwarz-Linek, V. A. Martinez, J. Arlt, A. N. Morozov, D. Marenduzzo, M. E. Cates, and W. C. K. Poon, Phys. Rev. Lett. **113**, 268101 (2014).

[9] R. Mok, J. Dunkel, and V. Kantsler, Phys. Rev. E **99**, 052607 (2019).

[10] L. Caprini and U. M. B. Marconi, Soft Matter **15**, 2627–2637 (2019).

[11] J. Palacci, S. Sacanna, A. P. Steinberg, D. J. Pine, and P. M. Chaikin, Science **339**, 936–940 (2013).

[12] B. M. Mognetti, A. Šarić, S. Angioletti-Uberti, A. Cacciuto, C. Valeriani, and D. Frenkel, Phys. Rev. Lett. **111**, 245702 (2013).

[13] A. P. Solon, J. Stenhammar, R. Wittkowski, M. Kardar, Y. Kafri, M. E. Cates, and J. Tailleur, Phys. Rev. Lett. **114**, 198301 (2015).

[14] I. Buttinoni, J. Bialké, F. Kümmel, H. Löwen, C. Bechinger, and T. Speck, Phys. Rev. Lett. **110**, 238301 (2013).

[15] I. Petrelli, P. Digregorio, L. F. Cugliandolo, G. Gonnella, and A. Suma, Eur. Phys. J. E **41**, 128 (2018).

[16] J. Bialké, T. Speck, and H. Löwen, J. Non-Cryst. Solids **407**, 367–375 (2015).

[17] M. N. Van Der Linden, L. C. Alexander, D. G. Aarts, and O. Dauchot, Phys. Rev. Lett. **123**, 098001 (2019).

[18] C. B. Caporusso, P. Digregorio, D. Levis, L. F. Cugliandolo, and G. Gonnella, Phys. Rev. Lett. **125**, 178004 (2020).

[19] F. Peruani, J. Starruß, V. Jakovljevic, L. Søgaard-Andersen, A. Deutsch, and M. Bär, Phys. Rev. Lett. **108**, 098102 (2012).

[20] S. Garcia, E. Hannezo, J. Elgeti, J.-F. Joanny, P. Silberzan, and N. S. Gov, Proc. Natl. Acad. Sci. U. S. A. **112**, 15314–15319 (2015).

[21] L. Caprini, U. M. B. Marconi, C. Maggi, M. Paoluzzi, and A. Puglisi, Phys. Rev. Res. **2**, 023321 (2020).

[22] S. Henkes, K. Kostanjevec, J. M. Collinson, R. Sknepnek, and E. Bertin, Nat. Commun. **11**, 1405 (2020).

[23] É. Fodor and M. Cristina Marchetti, Physica A **504**, 106–120 (2018).

[24] M. R. Shaebani, A. Wysocki, R. G. Winkler, G. Gompper, and H. Rieger, Nat. Rev. Phys. **2**, 181–199 (2020).

[25] G. Szamel, Phys. Rev. E **90**, 012111 (2014).

[26] S. Das, G. Gompper, and R. G. Winkler, New J. Phys. **20**, 015001 (2018).

[27] L. Caprini, U. M. B. Marconi, and A. Puglisi, Sci. Rep. **9**, 1386 (2019).

[28] K. Malakar, A. Das, A. Kundu, K. V. Kumar, and A. Dhar, Phys. Rev. E **101**, 022610 (2020).

[29] M. Hennes, K. Wolff, and H. Stark, Phys. Rev. Lett. **112**, 238104 (2014).

[30] S. Rana, M. Samsuzzaman, and A. Saha, Soft Matter **15**, 8865–8878 (2019).

[31] V. Holubec, S. Steffenoni, G. Falasco, and K. Kroy, Phys. Rev. Res. **2**, 043262 (2020).

[32] A. Militaru, M. Innerbichler, M. Frimmer, F. Tebbenjohanns, L. Novotny, and C. Dellago, Nat. Commun. **12**, 2446 (2021).

[33] S. C. Takatori, R. De Dier, J. Vermant, and J. F. Brady, Nat. Commun. **7**, 10694 (2016).

[34] O. Dauchot and V. Démery, Phys. Rev. Lett. **122**, 068002 (2019).

[35] R. Wittmann, C. Maggi, A. Sharma, A. Scacchi, J. M. Brader, and U. M. B. Marconi, J. Stat. Mech.: Theory Exp. **2017**, 113207.

[36] L. Caprini, F. Cecconi, A. Puglisi, and A. Sarracino, Soft Matter **16**, 5431–5438 (2020).

[37] D. Breoni, M. Schmiedeberg, and H. Löwen, Phys. Rev. E **102**, 062604 (2020).

[38] É. Fodor, C. Nardini, M. E. Cates, J. Tailleur, P. Visco, and F. van Wijland, Phys. Rev. Lett. **117**, 038103 (2016).

[39] U. M. B. Marconi, A. Puglisi, and C. Maggi, Sci. Rep. **7**, 46496 (2017).

[40] U. M. B. Marconi, M. Paoluzzi, and C. Maggi, Mol. Phys. **114**, 2400–2410 (2016).

[41] R. Wittmann and J. M. Brader, Europhys. Lett. **114**, 68004 (2016).

[42] R. Wittmann, F. Smallenburg, and J. M. Brader, J. Chem. Phys. **150**, 174908 (2019).

[43] P. Hänggi, P. Talkner, and M. Borkovec, Rev. Mod. Phys. **62**, 251 (1990).

[44] V. I. Melńikov, Phys. Rep. **209**, 1–71 (1991).

[45] A. Sharma, R. Wittmann, and J. M. Brader, Phys. Rev. E **95**, 012115 (2017).

[46] A. Geiseler, P. Hänggi, and G. Schmid, Eur. Phys. J. B **89**, 175 (2016).

[47] A. Scacchi and A. Sharma, Mol. Phys. **116**, 460–464 (2018).

[48] E. Woillez, Y. Zhao, Y. Kafri, V. Lecomte, and J. Tailleur, Phys. Rev. Lett. **122**, 258001 (2019).

[49] L. Caprini, U. M. B. Marconi, A. Puglisi, and A. Vulpiani, J. Chem. Phys. **150**, 024902 (2019).

[50] E. Woillez, Y. Kafri, and V. Lecomte, J. Stat. Mech.: Theory Exp. **2020**, 063204.

[51] Y. Fily, J. Chem. Phys. **150**, 174906 (2019).

[52] T. Debnath and P. K. Ghosh, Phys. Chem. Chem. Phys. **20**, 25069–25077 (2018).

[53] A. Scacchi, J. M. Brader, and A. Sharma, Phys. Rev. E **100**, 012601 (2019).

[54] A. Dhar, A. Kundu, S. N. Majumdar, S. Sabhapandit, and G. Schehr, Phys. Rev. E **99**, 032132 (2019).

[55] D. Wexler, N. Gov, K. Rasmussen, and G. Bel, Phys. Rev. Res. **2**, 013003 (2020).

[56] S. Gu, T. Qian, H. Zhang, and X. Zhou, Chaos **30**, 053133 (2020).

[57] E. Woillez, Y. Kafri, and N. S. Gov, Phys. Rev. Lett. **124**, 118002 (2020).

[58] S. Chaki and R. Chakrabarti, Soft Matter **16**, 7103–7115 (2020).

[59] G. Gradenigo and M. Paoluzzi, Chaos, Solitons Fractals **153**, 111500 (2021).

[60] M. Paoluzzi, D. Levis, and I. Pagonabarraga, arXiv:2109.14948 (2021).

[61] E. Tjhung and L. Berthier, Phys. Rev. Res. **2**, 043334 (2020).

[62] S. K. Nandi, R. Mandal, P. J. Bhuyan, C. Dasgupta, M. Rao, and N. S. Gov, Proc. Natl. Acad. Sci. U. S. A. **115**, 7688–7693 (2018).

[63] S. K. Nandi and N. S. Gov, Soft Matter **13**, 7609–7616 (2017).

[64] B. Walter, G. Pruessner, and G. Salbreux, Phys. Rev. Res. **3**, 013075 (2021).

[65] K. S. Olsen, L. Angheluta, and E. G. Flekkøy, Phys. Rev. Res. **2**, 043314 (2020).

[66] M. Paoluzzi, L. Angelani, and A. Puglisi, Phys. Rev. E **102**, 042617 (2020).

[67] A. Biswas, J. M. Cruz, P. Parmananda, and D. Das, Soft Matter **16**, 6138–6144 (2020).

[68]Z. Schuss, A. Singer, and D. Holcman, Proc. Natl. Acad. Sci. U. S. A. **104**, 16098–16103 (2007).

[69]E. Locatelli, F. Baldovin, E. Orlandini, and M. Pierno, Phys. Rev. E **91**, 022109 (2015).

[70]L. Caprini, F. Cecconi, and U. M. B. Marconi, J. Chem. Phys. **150**, 144903 (2019).

[71]P. K. Ghosh, J. Chem. Phys. **141**, 061102 (2014).

[72]L. Berthier, E. Flenner, and G. Szamel, New J. Phys. **19**, 125006 (2017).

[73]D. Mandal, K. Klymko, and M. R. DeWeese, Phys. Rev. Lett. **119**, 258001 (2017).

[74]L. Dabelow, S. Bo, and R. Eichhorn, Phys. Rev. X **9**, 021009 (2019).

[75]L. Caprini and U. M. B. Marconi, J. Chem. Phys. **154**, 024902 (2021).

[76]D. Martin, J. O'Byrne, M. E. Cates, É. Fodor, C. Nardini, J. Tailleur, and F. van Wijland, Phys. Rev. E **103**, 032607 (2021).

[77]G. Nguyen, R. Wittmann, and H. Löwen, J. Phys.: Condens. Matter **34**, 035101 (2022).

[78]L. Caprini and U. M. B. Marconi, Phys. Rev. Res. **2**, 033518 (2020).

[79]C. Maggi, M. Paoluzzi, A. Crisanti, E. Zaccarelli, and N. Gnan, Soft Matter **17**, 3807–3812 (2021).

[80]Y. Fily and M. C. Marchetti, Phys. Rev. Lett. **108**, 235702 (2012).

[81]T. F. Farage, P. Krinninger, and J. M. Brader, Phys. Rev. E **91**, 042310 (2015).

[82]L. Caprini, E. Hernández-García, C. López, and U. M. B. Marconi, Sci. Rep. **9**, 16687 (2019).

[83]X.-L. Wu and A. Libchaber, Phys. Rev. Lett. **84**, 3017 (2000).

[84]C. Maggi, M. Paoluzzi, N. Pellicciotta, A. Lepore, L. Angelani, and R. Di Leonardo, Phys. Rev. Lett. **113**, 238303 (2014).

[85]S. Chaki and R. Chakrabarti, Physica A **530**, 121574 (2019).

[86]P. Jung and P. Hänggi, Phys. Rev. A **35**, 4464 (1987).

[87]C. Maggi, U. M. B. Marconi, N. Gnan, and R. Di Leonardo, Sci. Rep. **5**, 10742 (2015).

[88]C. W. Gardiner, *Handbook of Stochastic Methods* (Springer, Berlin, 1985), Vol. 3.

[89]L. Dabelow, S. Bo, and R. Eichhorn, J. Stat. Mech.: Theory Exp. **2021**, 033216.

[90]L. Caprini, A. Puglisi, and A. Sarracino, Symmetry **13**, 81 (2021).

[91]S. Sato, J. Appl. Probab. **14**, 850–856 (1977).

[92]M. Rein and T. Speck, Eur. Phys. J. E **39**, 84 (2016).

[93]M. Asfaw and Y. Shiferaw, J. Chem. Phys. **136**, 025101 (2012).

[94]F. Cecconi, A. Puglisi, U. M. B. Marconi, and A. Vulpiani, Phys. Rev. Lett. **90**, 064301 (2003).

[95]D. B. Brückner, A. Fink, C. Schreiber, P. J. F. Röttgermann, J. O. Rädler, and C. P. Broedersz, Nat. Phys. **15**, 595–601 (2019).

[96]D. B. Brückner, A. Fink, J. O. Rädler, and C. P. Broedersz, J. R. Soc., Interface **17**, 20190689 (2020).

[97]A. Fink, D. B. Brückner, C. Schreiber, P. J. F. Röttgermann, C. P. Broedersz, and J. O. Rädler, Biophys. J. **118**, 552–564 (2020).

[98]L. Caprini and U. M. B. Marconi, J. Chem. Phys. **153**, 184901 (2020).

[99]S. Redner, *A Guide to First-Passage Processes* (Cambridge University Press, 2001).